# Thermo-Economic Analysis of a Geothermal-Based High Temperature Heat Pump

Pietro Ungar[1, *], Daniele Fiaschi[1], Giampaolo Manfrida[1]

[1]University of Florence, Department of Industrial Engineering, Florence, Italy

*Corresponding Author: pietro.ungar@unifi.it

## ABSTRACT

In light of growing environmental concerns, there's a heightened drive to lessen the industrial sector's reliance on natural gas. A system capable of providing mid-low temperature heat (ranging from 90°C to 120°C) in a sustainable and cost-effective way is increasingly attractive to the industrial sector. In this study, a detailed exergo-economic analysis of possible geothermal-based system has been performed to asses the economic feasibility of the proposed solution. Moreover, the performance of the sCO2-based system will be compared with a water loop for geothermal heat extraction coupled with an High-Temperature Heat Pump to asses the behaviour of the proposed scheme under different reservoir condition. In the scope of this study, it has been also considered the possibility of power cogeneration which could be achieved, for the sCO2-based system, exploiting the natural pressurisation of the fluid due to the thermosyphon effect, and that will be even more appealing for the industrial sector.

## 1 Introduction

Efficient production and distribution of renewable energy are key challenges to reaching the net-zero target by 2050. Particularly, in 2021, heat production accounted for half of the total energy consumption in the world (IEA (2022)), 51% of which was required from industrial processes, which commonly need a heat temperature above 80°C (IEA-IETS (2014)). In addition, according to a work published in 2019 by the Oxford Study for Energy Studies, industrial processes requiring heat in the temperature range of 100°C – 500°C represent 30% of the total industrial heat requirements and are connected mainly with paper and print, food, and chemical processes (Honore (2019)). HTHP (High Temperature Heat Pumps) are one of the most promising technologies for the decarbonization of industrial heat demand. For this reason, in recent years there has been a growing scientific interest in the field.

### 1.1 High-Temperature Heat Pumps

Arpagaus et al., 2018 (Arpagaus et al. (2018)), did a very extensive review of the actual market and state of art of high-temperature heat pumps, highlighting the need for the progressive development of HTHP with a delivery temperature of over 140°C. A detailed analysis of the possible configurations for those applications has been published by Zühlsdorf et Al. in 2019 (Zühlsdorf et al. (2019)). In their paper, they focus on the production of steam for industrial application analyzing two different HTHP configurations which have proven to be competitive, in terms of levelized cost of heat, with other technologies. According to the authors of this study, the most promising cycles for industrial steam production are a steam compression system and a sCO2 reversed Bryton cycle. These cycles, slightly modified for integration with the geothermal system, have been analyzed in this study. As pointed out by Asparagus (Arpagaus et al. (2018)), the efficiency of an HTHP system is directly related to the source temperature, hence coupling the heat pump with a geothermal system could be extremely beneficial in terms of energy consumption.

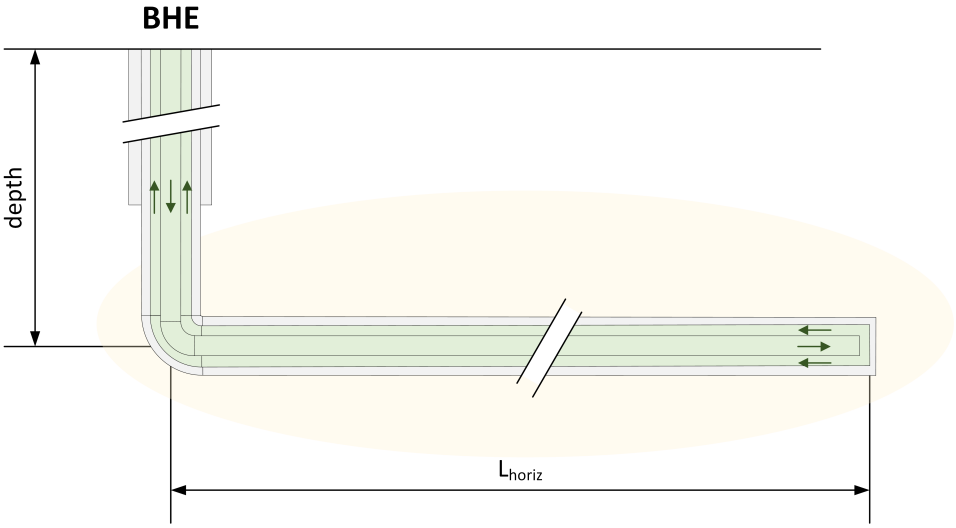


**Figure 1:** Schemes of a concentric BHE well

### 1.2 Well Model

Multiple models for geothermal wells have been considered throughout the years, in this work we have focused in analysing the behaviour of a closed loop borehole heat exchanger (BHE). The considered well, sketched in Figure 1, is composed of two concentric pipes in which the fluid is circulated and heated up by exchanging heat with the surrounding rocks. This kind of well has been extensively studied in recent years by multiple researchers both in its vertical (Sun et al. (2018a) and Galoppi et al. (2015)) or horizontal (Sun et al. (2018b)) configuration. Recently, an European project has been awarded for enhancing the development of this kind of wells (European Project (2022)).

### 1.3 Analysed Configurations

Two different surface installation schemes have been considered for this analysis (as shown in Figure 2). The water-based scheme is simpler and has been used just for benchmarking the $CO_2$-based result. In this particular configuration, the water, heated in the well, is used to power the evaporator of an high temperature heat pump and then directly re-injected in the well to be heated up again.

The $CO_2$-based scheme, on the other hand, is slightly more complex: the $CO_2$ is injected into the well as saturated liquid. The heated and compressed $CO_2$ is then mixed with the $CO_2$ vapour that could be accumulating in the separator and then compressed to reach the desired temperature level ($T_{max}$). The $CO_2$ is then cooled down in the main heat exchanger (providing power to the heat pump users) and then expanded to recover part of the compressor power. Before the expansion there's the possibility of further cooling the $CO_2$ to decrease the quality of the $CO_2$ coming out from the turbine.

## 2 Methodology

### 2.1 Thermodynamic Model

To evaluate the behaviour of these systems two different sub-models have been developed: the model of the well and the model of the surface installation.

**2.1.1 Well Model** The model developed by Ungar in his PhD thesis (Ungar (2023)) has been used to predict the behaviour of the fluid inside the well. The model works by integrating the momentum (eq.1) and energy (eq.2) balance equation tough-out the well.

$$\frac{dp}{dl} = -\left(\rho g cos\theta + dp_{loss}\right) \tag{1}$$

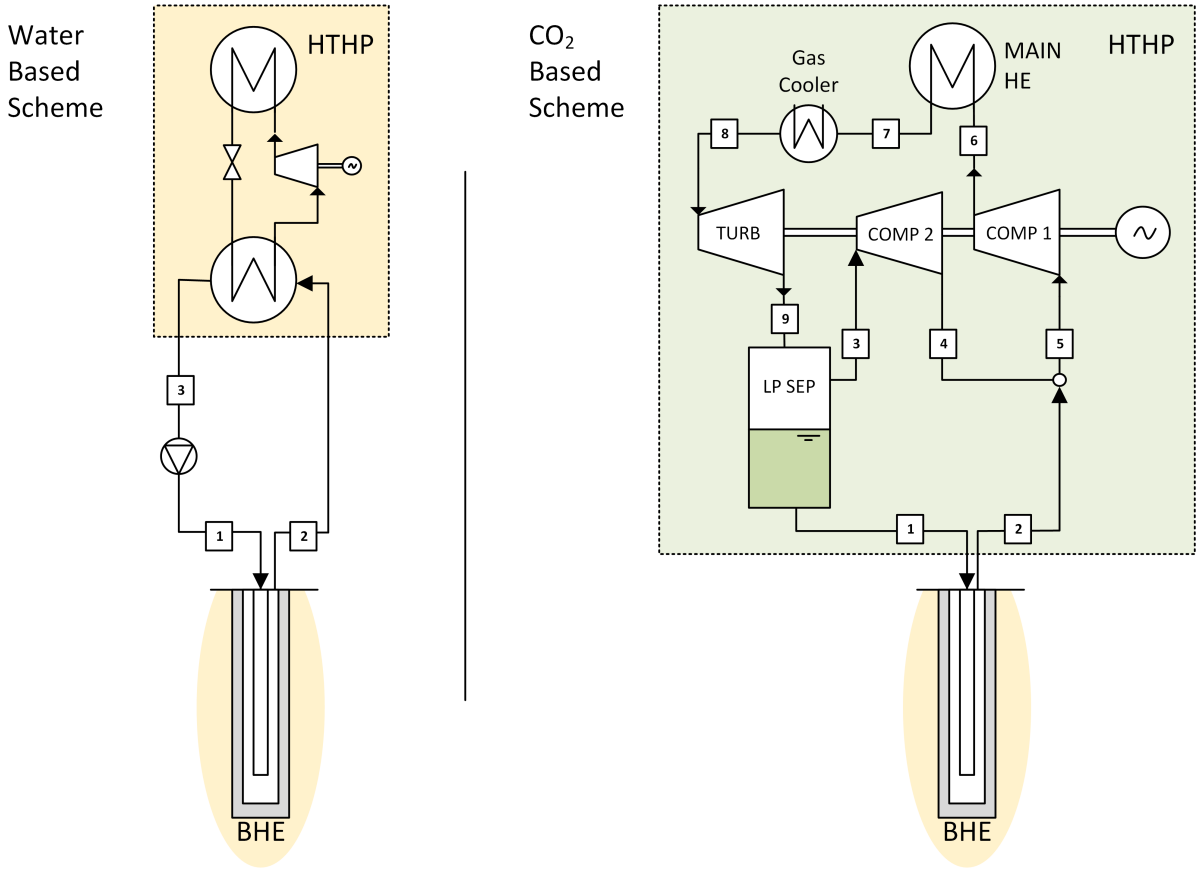


**Figure 2:** Schemes considered for the analysis. Left: Water-based system coupled with an high temperature heat pump, Right: $CO_2$-based system

$$\frac{dh}{dl} = -\left(gcos\theta \; - d\dot{q}_{tot}/\dot{m}_{well}\right) \tag{2}$$

where $\theta$ is the inclination of the well with respect to the vertical direction, $\dot{m}_{well}$ is the flow rate of teh fluid inside the well, $d\dot{q}_{tot}$ and $dp_{loss}$ are the derivative heat exchanged and pressure losses of the fluid.

The system composed of (1) and of (2) is integrated in python using a explicit 5th order Runge-Kutta method (Dormand and Prince (1980)) as implemented in the SciPy python package (Virtanen et al. (2020)).

The pressure losses are evaluated using the Churchill correlation (Churchill (1977)) for the estimation of friction factor $f$:

$$dp_{loss} = f\frac{1}{2\rho d_h}\left(\frac{\dot{m}_{well}}{A_{flow}}\right)^2 \tag{3}$$

To account for heat transfer in rocks formation around the well without having to solve a finite difference model of the temperature distribution in the surrounding, a semi-analytical correlation has been implemented (Zhang et al. (2011)):

$$R_{rocks} = \frac{d_{well}}{2k_{rocks}f(t_d)} \tag{4}$$

with:

$$f(t_d)_{base} = \begin{cases} \frac{1}{2} + (\pi t_d)^{-\frac{1}{2}} - \frac{1}{4}\left(\frac{t_d}{\pi}\right)^{\frac{1}{2}} + \frac{1}{8}t_d, & \text{if } t_d < 2.8 \\ \frac{2}{ln(4t_d)-2\gamma} - \frac{2\gamma}{(ln(4t_d)-2\gamma)^2}, & \text{if } t_d \geq 2.8 \end{cases} \tag{5}$$

Where, in (5):

- $t_d = 4\alpha_{rocks}t/d^2_{well}$ is a dimensionless time ($t$ in seconds)
- $\alpha_{rocks} = k_{rocks}/\rho_{rocks}C_{p_{rocks}}$ is the thermal diffusivity of the rocks
- $\gamma$ is Euler's constant
- $d_{well}$ is the external diameter of the well

To keep the water-based and the $CO_2$-based solutions comparable, the same well has been considered for both. The main design parameter are listed in the table below:

**Table 1:** Geothermal BHE design parameters

| Symbol | Description | Value |
|---|---|---|
| $well_{depth}$ | Depth of the horizontal section | 3km |
| $well_{lenght}$ | Overall length of the well | 6.5km |
| $\Phi_{cas_{id}}$ | External diameter of the annulus | 16cm |
| $\Phi_{tub_{od}}$ | Internal diameter of the annulus | 13cm |
| $\Phi_{tub_{id}}$ | Internal diameter of the tubing | 10cm |

The geothermal gradient of the rocks around the well ($\nabla T_{geo}$) has been varied to test different geological conditions. The flow rate that circulates inside the well ($\dot{m}_{well}$) has been varied as well.

**2.1.2 $CO_2$-Based Heat Pump Model** The $CO_2$-based heat pump model has been developed in EES (Klein (2020)). The pressure at the outlet of the main compressor *(*COMP 1 *in Figure 2)* is adjusted according to the inlet condition to reach the desired temperature in point 6 *($T_{max}$)*. The temperature at the inlet of the turbine *($T_{turb_{in}}$)* is an important parameter as well and can be optimised. In fact, lowering $T_{turb_{in}}$ result in a decreased turbine power output but it will also decrease the amount of vapour that has to be re-compressed trough the compressor *COMP 2*.

Some fixed parameters were assumed in the model. They are listed in the table below:

**Table 2:** $CO_2$-based HTHP - Fixed Parameters

| Symbol | Description | Value |
|---|---|---|
| $\eta_{comp}$ | Compressor Efficiency | 0.8 |
| $\eta_{turb}$ | Turbine Efficiency | 0.75 |
| $dT_{main\ HE}$ | Temperature range inside the main heat exchanger | 40°C |
| $T_{sat}$ | Saturation Temperature in the low pressure separator *(LP SEP)* | 10°C |

**2.1.3 Water-Based Heat Pump Model** Following the approach described in (Ungar et al. (2023)), the heat pump connected to the water-based well has been modelled considering a fixed exergy efficiency of 0.4, which has been chosen based on some experimental results from literature (Bilgen and Takahashi (2002)). Knowing the exergy efficiency is possible to estimate the electrical power demand as:

$$\dot{W}_{HP} = \frac{1}{\eta_{exergy}}\left(1 - \frac{T_{low}}{T_{high}}\right)\dot{Q}_{HP} = \frac{1}{0.4}\left(1 - \frac{T_{low}}{T_{high}}\right)\dot{Q}_{HP} \tag{6}$$

Where $T_{low}$ has been supposed to be equal to $T[3]$ (the index refers to Fig 2) and hence depends on the water temperature range in the HE which can be optimised (a lower temperature in 3 means an higher heat extraction rate from the well but also requires some additional work from the heat pump which has to overcome an higher temperature difference).

Once both models have been solved an exergy analysis have been conducted using an in-house developed tool called *"3ETool"* (Fiaschi et al. (2022)).

**2.1.4 Economic Analysis** The Levelized Cost of Heat (LCOH) has been evaluated for both the solutions following the same approach described in a previous paper (Ungar et al., 2023):

$$LCOH = \frac{C_{tot}\beta + \dot{W}_{tot}c_{el}}{\dot{Q}_{DH}}, \quad \beta = \frac{1 + \alpha OM_{ratio}}{\alpha h_y}, \quad \alpha = \frac{1 - (1+i)^{-L_e}}{i} \tag{7}$$

With $\dot{W}_{tot}$ being the net electrical power required to run the system (or sold to the grid if the conditions allow for co-generation) and $\dot{Q}_{DH}$ the power delivered to the heat user. In addition, $C_{tot}$ is the overall investment cost to setup the system, $c_{el}$ the cost of electricity, $C_{om}$ the operation an maintenance cost ($C_{om} = OM_{ratio}C_{tot}$, with $OM_{ratio} = 5\%/year$). Finally, $L_e = 20years$ is the expected lifetime of the plant, $i = 4\%/year$ is the interest rate and $h_y = 8000hours/year$ is the expected operational time of the system, that are reasonable values if an industrial application is considered.

$C_{tot}$ is evaluated differently for the water-based and the $CO_2$-based systems:

$$C_{tot_{H_2O}} = C_{well} + C_{HP} \tag{8}$$

$$C_{tot_{CO_2}} = C_{well} + C_{turb} + \sum C_{comp} + \sum C_{HE} \tag{9}$$

The different correlations that have been used to estimate the cost of the system components are listed in Table 3 (in the appendix).

## 3 Results

### 3.1 Well Behaviour

The well behaves very differently between the water-based and $CO_2$-based scenario. As shown in Figure 3, in the water-based case, the pressure decrease inside the well due to the pressure losses while in the $CO_2$-based case there's an important pressure increase inside the well. This is due to the fact that, in the horizontal section of the well, the $CO_2$ while heating up, decrease it's density resulting in a significant thermosyphon effect. The temperature increase and the overall output power is comparable between the two configurations.

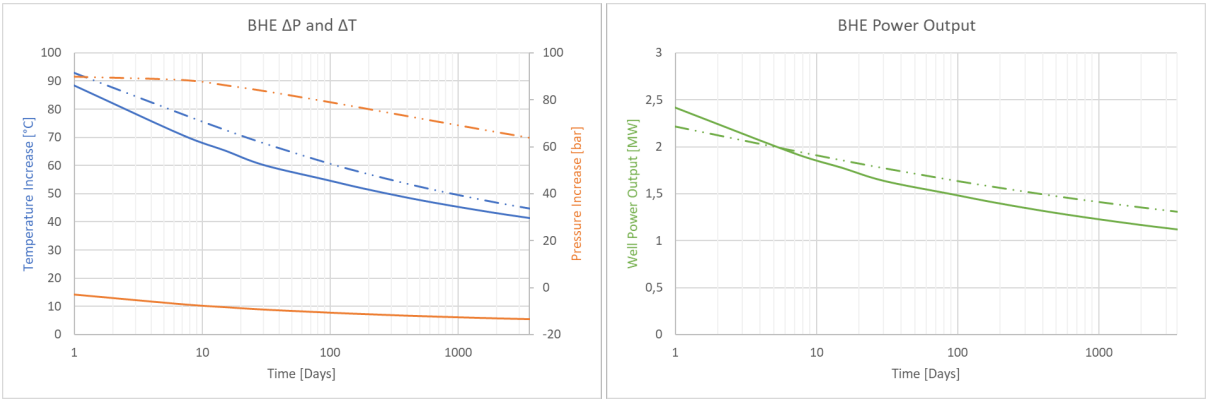


**Figure 3:** Comparison between water-based *(dash-dotted line)* and $CO_2$-based *(plain line)* well behaviour. *Left:* Temperature and Pressure increase with time. *Right:* Well power output with time. *(Conditions: $\nabla T_{geo}$=50°C/km, $T_{sat}$=10°C, $T_{water_{in}}$=45°C)*

Another interesting thing to notice is the effect of different geothermal gradients on the $CO_2$ behaviour. As shown in Figure 4, the outlet pressure decrease with time for lower gradients while the opposite happens for $\nabla T_{geo}$=75°C/km.

This can be explained looking at Figure 5, which shows the profile of the fluid temperature and pressure inside the well.

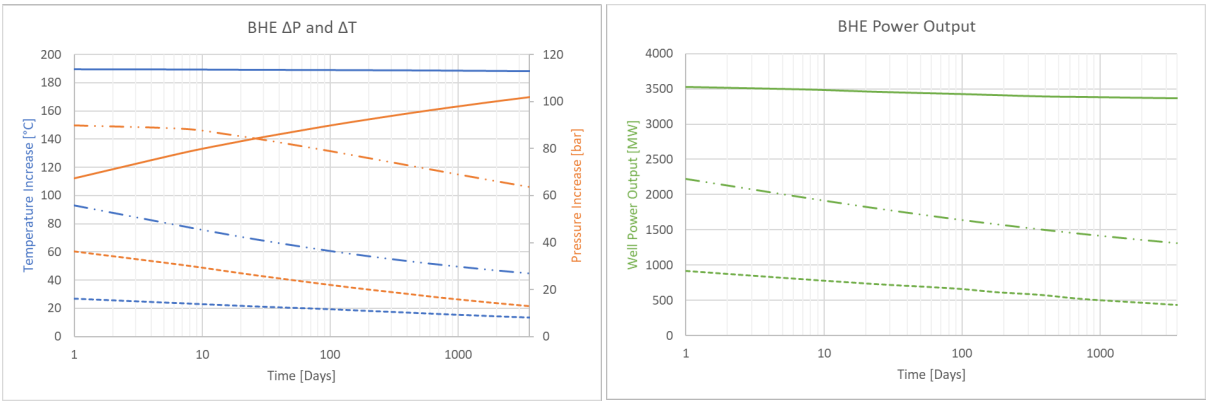


**Figure 4:** $CO_2$-based well behaviour. *Left:* Temperature and Pressure increase with time. *Right:* Well power output with time. Plain line: $\nabla T_{geo}$=75°C/km, Dash-dotted line: $\nabla T_{geo}$=50°C/km, Dashed line: $\nabla T_{geo}$=25°C/km *(Condition: $T_{sat}$=10°C)*

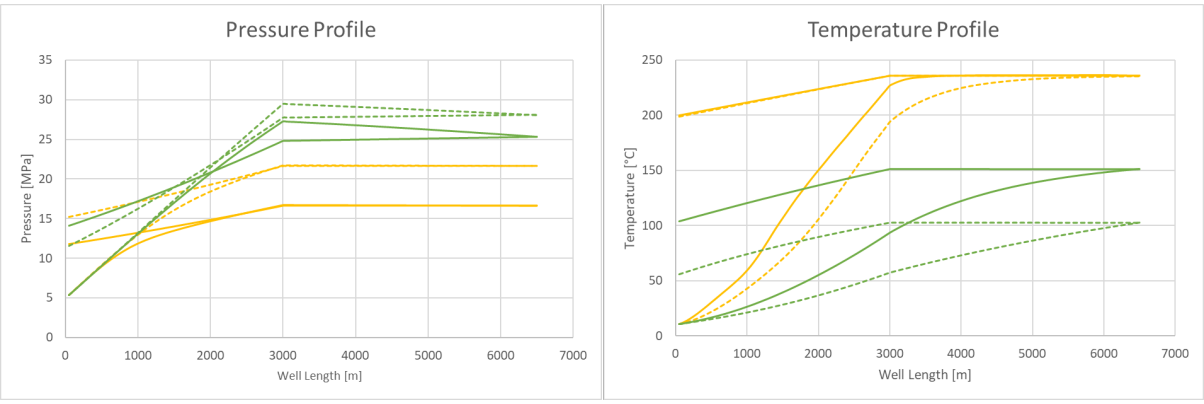


**Figure 5:** Pressure and Temperature profile inside the well for different geothermal gradient and times. *Plain line: $t$ = 1$year$ $\nabla T_{geo}$=75°C/km, dash-doted line $\nabla T_{geo}$=50°C/km, dashed line $\nabla T_{geo}$=25°C/km*

For the $\nabla T_{geo}$=75°C/km case, outlet pressure increase with time because the $CO_2$ will heat up less while descending into the vertical section of the well resulting in an denser fluid at horizontal section inlet and hence a stronger thermosyphon effect. On the other hand, for the $\nabla T_{geo}$=50°C/km case, the effect of a denser $CO_2$ at the inlet of the horizontal section is mitigated by the greater reduction in outlet temperature which result in a denser ascending fluid.

### 3.2 HTHP Behaviour

Regarding the HTHP, an example of its thermodynamic behaviour is depicted in Figure 6. The $CO_2$ is injected into the well as saturated liquid at a specific $T_{sat}$ *(Point 1)*. It is then usually extracted from the well as a supercritical fluid, pressurised and heated up *(Point 2)*, mixed with the incoming re-compressed flash vapour from the separator *(points 3, 4 and 5)*, and compressed, if needed to reach the desired temperature level *(Point 6)*. The fluid is then cooled down to extract useful heat and then further cooled down to a specific temperature ($T_{turb_{in}}$) to decrease the vapour quality at the outlet of the expander.

As can be seen from Figure 8, the net power outlet, defined as in equation 10, usually increase with decreasing $T_{turb_{in}}$. This is because the specific work needed by the flash vapour re-compression ($\dot{w}_{comp2}$) is significantly higher to both the specific work of the turbine and of the HP compressor thus is imperative to avoid vapour generation in the expander as much as possible.

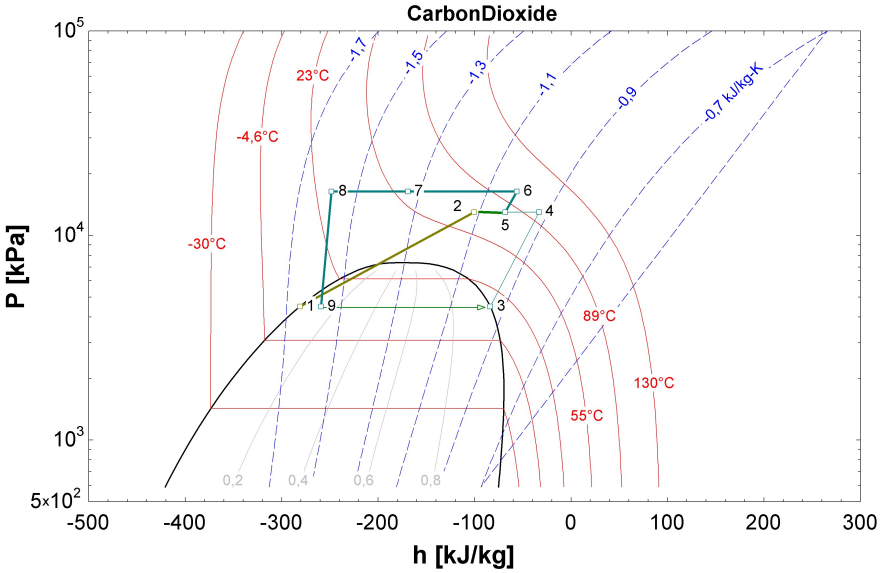


**Figure 6:** Depiction of the thermodynamic behaviour of the $CO_2$-based system from Figure 2 *(Considered condition: $T_{max}$=100°C, $T_{turb_{in}}$=30°C, $well_{depth}$=2km, $well_{lenght}$=6.5km, $\nabla T_{geo}$=50°C/km, t=180days)*

$$\dot{W}_{net} = \dot{W}_{turb} - \dot{W}_{comp1} - \dot{W}_{comp2} \tag{10}$$

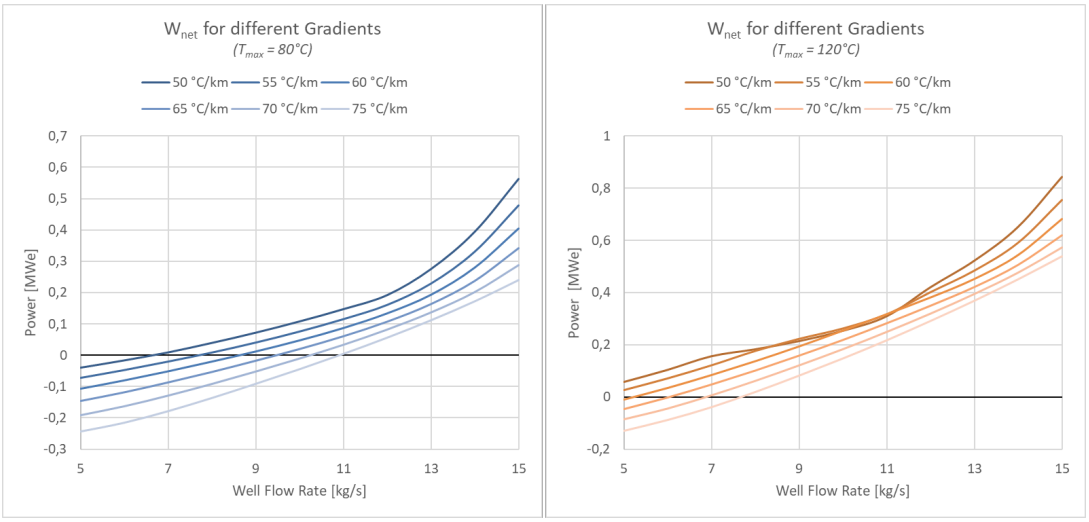


**Figure 7:** Effect of $\dot{m}_{well}$ on the $CO_2$-based system behaviour *(Considered condition: $T_{max}$=80°C, $well_{depth}$=3km, $well_{lenght}$=6.5km, t=10years)*

Is interesting to notice that, in the condition depicted in Figure 8, with lower flow rates circulated into the well there could be the possibility to achieving some co-generation, highlighted by negative power requirements, even considering an higher supply temperature which is something that water based system can not do.

### 3.3 Economic Analysis

Finally, by comparing the LCOH results from water and $CO_2$-based systems, it appears clearly that water based systems are more suitable for being used for providing heat when higher geothermal gradients are

present, while $CO_2$ can be an useful tool to provide sustainable heat even in regions with lower geothermal gradients.

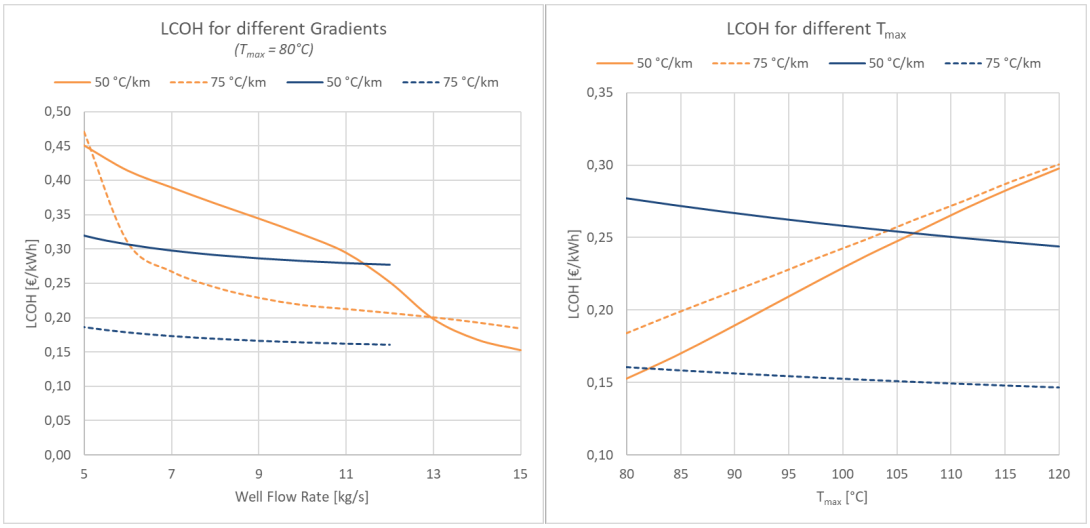


**Figure 8:** Comparison of the LCOH result for the water-based (blue lines) and $CO_2$-based (orange lines) systems *(Considered condition: $well_{depth}$=3km, $well_{lenght}$=6.5km, t=10years)*

The LCOH achieved with these kind of wells are usually high do to the high investment cost needed for well drilling (the considered well is expected to cost around 11M€). Despite this, the resulting LCOH are comparable with the ones obtained by other comparable technologies like pellet boilers (around 15c€/kWh) and solar thermal (around 10c€/kWh) (source: IEA, 2024)

## 4 Conclusion

In conclusion is possible to say the usage of $CO_2$ as a working fluid for closed loop wells, as the one analysed in this paper, is a promising source of reliable low temperature heat (less than 100°C) especially for lower geothermal gradients. The predicted LCOH is high, which is something that could be expected given the nature of the closed loop geothermal wells, but at least comparable with some existing technologies making the proposed solution one of the possible option of choice for the transition of the heating sector.

## Acknowledgments

This research is part of the contribution of the University of Florence to the HOCLOOP project (Grant agreement ID: 101083558)

## References

Adams, B. M. et al. (2021). “Estimating the Geothermal Electricity Generation Potential of Sedimentary Basins Using genGEO (the generalizable GEOthermal techno-economic simulator)”. In: *ChemRxiv Preprint*.

Arpagaus, C. et al. (June 2018). “High temperature heat pumps: Market overview, state of the art, research status, refrigerants, and application potentials”. In: *Energy* 152, pp. 985–1010. ISSN: 03605442. DOI: 10.1016/j.energy.2018.03.166.

Bilgen, E. and H. Takahashi (Jan. 2002). “Exergy analysis and experimental study of heat pump systems”. In: *Exergy, An International Journal* 2.4, pp. 259–265. ISSN: 11640235. DOI: 10.1016/S1164-0235(02)00083-3.

Churchill, S. W. (1977). “Friction-factor equatin spans over all fluid-flow regimes”. In: *Chemical Engineering* 84, pp. 91–92.

Dormand, J. and P. Prince (Mar. 1980). "A family of embedded Runge-Kutta formulae". In: *Journal of Computational and Applied Mathematics* 6.1, pp. 19–26. ISSN: 03770427. DOI: 10.1016/0771-050X(80)90013-3.

European Project (2022). *A circular by design environmentally friendly geothermal energy solution based on a horizontal closed loop - HOCLOOP*.

Fiaschi, D. et al. (2022). "Development of an exergo-economic and exergo-environmental tool for power plant assessment: evaluation of a geothermal case study". In: *34th International Conference on Efficiency, Cost, Optimization, Simulation and Environmental Impact of Energy Systems (ECOS 2021)*. Tokyo, Japan: ECOS 2021 Program Organizers, pp. 24–35. ISBN: 978-1-7138-4398-6. DOI: 10.52202/062738-0003. URL: http://www.proceedings.com/062738-0003.html.

Galoppi, G. et al. (Dec. 2015). "Feasibility Study of a Geothermal Power Plant with a Double-pipe Heat Exchanger". In: *Energy Procedia* 81, pp. 193–204. ISSN: 18766102. DOI: 10.1016/j.egypro.2015.12.074.

Honore, A. (May 2019). *Decarbonization and industrial demand for gas in Europe*. Tech. rep. Oxford, United Kingdom: Oxford Institute for Energy Studies. DOI: 10.26889/9781784671396.

IEA (2022). *Heating*.

– (2024). *Levelized cost of heating (LCOH) for consumers, for selected space and water heating technologies and countries*. URL: https://www.iea.org/data-and-statistics/charts/levelized-cost-of-heating-lcoh-for-consumers-for-selected-space-and-water-heating-technologies-and-countries.

IEA-IETS (2014). *Application of Industrial Heat Pumps*. Tech. rep.

Klein, S. (June 2020). *EES – Engineering Equation Solver*.

Pieper, H. et al. (Aug. 2018). "Allocation of investment costs for large-scale heat pumps supplying district heating". In: *Energy Procedia* 147, pp. 358–367. ISSN: 18766102. DOI: 10.1016/j.egypro.2018.07.104.

Sun, F. et al. (Sept. 2018a). "Geothermal energy extraction in CO2 rich basin using abandoned horizontal wells". In: *Energy* 158, pp. 760–773. ISSN: 03605442. DOI: 10.1016/j.energy.2018.06.084.

– (Sept. 2018b). "Performance of geothermal energy extraction in a horizontal well by using CO2 as the working fluid". In: *Energy Conversion and Management* 171, pp. 1529–1539. ISSN: 01968904. DOI: 10.1016/j.enconman.2018.06.092.

Ungar, P. (Mar. 2023). "Use of CO2 as working fluid in geothermal systems". PhD thesis. Florence: University of Florence.

Ungar, P. et al. (2023). "Thermo-Economic Comparison of CO2 and Water as a Heat Carrier for Long-Distance Heat Transport from Geothermal Sources". In: *36th International Conference on Efficiency, Cost, Optimization, Simulation and Environmental Impact of Energy Systems (ECOS 2023)*. Las Palmas De Gran Canaria, Spain: ECOS 2023, pp. 2593–2602. ISBN: 978-1-7138-7492-8. DOI: 10.52202/069564-0233.

Virtanen, P. et al. (Mar. 2020). "SciPy 1.0: fundamental algorithms for scientific computing in Python". In: *Nature Methods* 17.3, pp. 261–272. ISSN: 1548-7091. DOI: 10.1038/s41592-019-0686-2.

Weiland, N. T., B. W. Lance, and S. R. Pidaparti (June 2019). "sCO2 Power Cycle Component Cost Correlations From DOE Data Spanning Multiple Scales and Applications". In: *ASME Turbo Expo 2019: Turbomachinery Technical Conference and Exposition*. Phoenix, Arizona, USA: American Society of Mechanical Engineers. ISBN: 978-0-7918-5872-1. DOI: 10.1115/GT2019-90493.

Zhang, Y. et al. (2011). "A time-convolution approach for modeling heat exchange between a wellbore and surrounding formation". In: *Geothermics* 40.4, pp. 261–266. ISSN: 03756505. DOI: 10.1016/j.geothermics.2011.08.003.

Zühlsdorf, B. et al. (Apr. 2019). "Analysis of technologies and potentials for heat pump-based process heat supply above 150°C". In: *Energy Conversion and Management: X*. ISSN: 25901745. DOI: 10.1016/j.ecmx.2019.100011.

## Appendix - Cost Correlation Table

**Table 3:** Cost correlation used in economic analysis

| Comp. | Cost Correlation | Notes |
|---|---|---|
| Well | $C_{well} = a\left(0.105{L_{well}}^2 + 1776 L_{well}\Phi_{cas_{id}} + 2.735E5\right)$ | *Result in [$], well diameter ($\Phi_{cas_{id}}$) and length ($L_{well}$) in [m], a = is a coefficient accounting for cost actualisation other uncertainties which is better detailed in the source (Source: Adams et al., 2021)* |
| Heat Exchangers | $C_{HE} = 49.45{UA_{HE}}^{0.7544}$ | *Result in [$], Correlation for $CO_2$, $UA_{HE}$ in [W/K], it is the product of the HE area and heat transfer coefficient (Source: Weiland et al., 2019)* |
| Compr. | $C_{comp} = 1230000\dot{W}_{comp}^{0.3992}$ | *Result in [$], Correlation for $CO_2$, $\dot{W}_{comp}$ in [MW], is the compressor power (Source: Weiland et al., 2019)* |
| Turbine | $C_{turb} = 406200\dot{W}_{turb}^{0.8}$ | *Result in [$], Correlation for $CO_2$, $\dot{W}_{turb}$ in [MW], is the turbine power (Source: Weiland et al., 2019)* |
| Heat Pump (Water) | $C_{HP} = 0.33667\dot{W}_{HP}$ | *Result in [M€], $\dot{W}_{HP}$ in [MW], Correlation for $\dot{W}_{HP}$ up to 10MW, Only the heat pump acquisition cost has been considered. (Source: Pieper et al., 2018)* |